

林 为 干

微波场论

与应用研究论文选集

LIN WEIGAN'S SELECTED WORKS
IN MICROWAVE FIELD THEORY
AND APPLICATION STUDY

電子工業出版社

204

1

林为干微波场论与应用研究论文选集

LIN WEIGAN' S SELECTED WORKS IN MICROWAVE
FIELD THEORY AND APPLICATION STUDY

電子工業出版社

内容简介

本论文选集收集了著名微波科学家,中国科学院学部委员林为干教授近 40 年来在国内外一级刊物上发表的具有国际先进科学水平的微波场论与应用研究论文 40 余篇。内容包括七大部分:(1)一腔多模微波电路理论与应用;(2)传输线函数理论解;(3)含不均匀介质的波导传输理论的研究;(4)非圆介质光波导的平均取值法;(5)波导不连续性的等数电路(6)小孔耦合理论的应用(7)综合研究。

本论文选集可供高等院校师生和有关科技人员阅读。

林为干微波场论与应用研究论文选集
LIN WEIGAN' S SELECTED WORKS
IN MICROWAVE FIELD THEORY AND APPLICATION STUDY
责任编辑 王昌铭

*

电子工业出版社出版(北京海淀区万寿路)
电子工业出版社发行 各地新华书店经售
北京顺义李史山印刷厂印刷

*

开本:787×1092毫米 1/16 印张:22.5 字数:547千字
1989年10月第一版 1989年10月第一次印刷
印数:1—1,500册 定价:12.00元
ISBN7-5053-0700-2/TN·255

序 言

我国著名的电子学科学家林为干教授是我结识多年的老朋友、一位出色的微波专家。他于1939年毕业于清华大学,曾赴美在科罗拉多州大学当研究生。1946年后在加利福尼亚大学(伯克利)当过研究生、助教、讲师,1950年获得博士学位,其论文“单腔多模微波滤波器”,深受微波界的重视。1951年他怀着满腔的爱国热情回到祖国,先后在岭南大学、中山大学、华南工学院任教。从1957年至今,他一直在成都电讯工程学院(现名电子科技大学)从事教学和科研工作。40多年来,他为我国和美国培养了二十名博士研究生和四十名硕士研究生;在国内外学术期刊杂志上发表了近百篇论文,著有《微波网络》、《微波理论与技术》、《电磁场工程》以及《电磁场理论》等专著,对微波理论与技术以及激光传输理论的发展和应用作出了重大贡献,得到了国内外专家、学者的赞誉。

本书将林为干教授花了几十年的心血发表的主要论文收集汇编出版,是一件可喜之事,我非常赞同。书中七个部分基本上概括了林为干教授多年来主要的学术见解和重大贡献,使读者能较系统地领会其精湛的学术思想。

从书中我们可看到:

他首先发现了圆柱谐振腔中存在着二、三、四、五个简并模,利用简并耦合,一个谐振腔可具有二个、三个、四个、五个单腔的电路功能。他第一次建立的一腔五膜微波滤波器,曾发表于美国应用物理杂志(1951年),根据该理论制成的单腔多模滤波器和纸张测湿仪已得到广泛的应用。

他在传输函数的研究方面还独树一帜,发表了许多具有国际水平的文章。他与钟祥礼教授共同发表的论文“传输线特性阻抗的一个新的计算方法”(物理学报1963年),被国外学者称为“林、钟方法”、是“至今最准确的方法”。

1979年他在椭圆直波理论的研究方面也取得了重大成就,纠正了国外的结论,成功地为我国制订椭圆直波导标准尺寸提供了依据。他对介质波导的深入研究,使我国激光传输理论达到了国际先进水平。

在其它方面,他也作了不少工作,读者将从本书中得到教益。

我虽然和林为干教授接触时间不多,但他严谨的治学学风和求实的科学态度给我留下了深刻的印象。我相信,本书将是我国微波科学界的宝贵财富,对我国科学事业,特别是对微波理论及传输技术的发展有重大的促进作用,同时,也能激励中青年学者学习林为干教授,为振兴中华贡献自己的一切力量。

孙俊人

1989. 8. 28



著名电子学科学家林为干博士生于1919年10月20日,中国广东省台山县人,1939年毕业于中国国立清华大学(昆明),1947年6月和1950年6月在美国伯克利加州大学分别获硕士学位和博士学位。

林为干博士于1947年9月至1948年6月在美国伯克利加州大学任助教,1948年9月至1951年6月任该校讲师。1951年回中国后任教授。现任电子科技大学教授,中国科学院学部委员。

林为干博士于1981年冬季任美国伯克利加州大学 *EECS* 系客座教授;1981年4月至6月在美国华盛顿任乔治华盛顿大学客座著名研究员。1981年3月选为中国科学院学部委员。1981年至1984年任成都电讯工程学院(现电子科技大学)副院长。1984年9月至12月任加拿大 *Manitoba* 大学客座教授。1984年9月起至今任中国电子学会微波专业委员会主席;1986年9月至今任美国电气电子工程师协会(*IEEE*)微波理论与技术学会(*MTT*)中国分会主席。

林为干教授长期从事的教学和研究领域是电磁理论,微波理论、微波网络、光波导理论和天线理论等。

Distinguished electronic Scientist, prof Weigan Lin was born in Canton, China, Oct. 20, 1919 and graduated from National Tsing Hua University, Kuming, China. He received the M. S. and Ph. D. degrees in June 1947 and June 1950, respectively, from the University of California, Berkeley.

From September 1947 to June 1948, he was a Teaching Assistant, and from September 1948 to June 1951, he was a Lecturer in electrical engineering at the University of California, Berkeley. Since September 1951, he has been a Professor in the People's Republic of China and is now at the Chengdu Institute of Radio Engineering, Chengdu, Sichuan, People's Republic of China. In the winter quarter of 1981, he was a Visiting Professor, EECS Department, University of California, Berkeley, CA. From April to June 1981, he was a Visiting Distinguished Scholar at George Washington University, Washington, DC. In March 1981, he was elected a Member of the Academy of Sciences of China (Academia Sinica). From 1981 to 1984, he held the position of Vice-President of the Chengdu Institute of Radio Engineering (Now, the University of Electronic Science and Technology of China, Chengdu, 610054, China). His field of teaching interest and research is in electromagnetic theory, microwave theory, microwave networks, optical waveguide theory, and antenna theory. He was Visiting Professor at the University of Manitoba, Canada, from September to December 1984.

Dr. Lin is a member of Sigma Xi and is Chairman of the Society of Microwaves, Chinese Institute of Electronics, since September 1984 and Chairman, IEEE Microwave Theory and Techniques, Beijing Chapter Since September, 1986.

目 录

第一部分 一腔多模微波电路理论与应用.....	(1)
1. Microwave Filters Employing a Single Cavity Excited in More than One Mode	(1)
2. ORTHOGONAL MODES IN A RECTANGULAR CAVITY	(12)
3. 正三角形简并式波导滤波器	(26)
第二部分 传输线函数理论解	(34)
1. Computation of the Parallel-Plate Capacitor with Symmetrically Placed Unequal Plates	(34)
2. CONTRIBUTIONS TO THE THEORY OF ELLIPTICAL WAVEGUIDES	(42)
3. POWER CARRYING CAPACITY REDUCTION IN STRAIGHT REGULAR WAVEGUIDE CONTAINING FOREIGN CONDUCTING BODIES	(55)
4. Polygonal Coaxial Line with Round Center Conductor	(67)
5. A New Transmission Line of Round Conductor and Parallel Plate with Symmetrically Placed Slit	(71)
6. 具有矩形柱内导体圆柱外导体的同轴线的特性阻抗	(73)
7. 扇形、椭圆、半椭圆波导的研究	(78)
8. 由已知相应的静电静磁问题求电动力学问题的解	(95)
9. 一类经典静电问题的解及其新的应用	(111)
10. CHARACTERISTIC IMPEDANCES OF THE SLOTTED COAXIAL LINE	(119)
11. 几个三角形波导的振幅分布函数	(127)
12. Step and Taper Waveguide Section with Rounded Corners	(136)
13. 传输线特性阻抗的一个新计算方法	(147)
14. 椭圆外导体-矩形内导体同轴线的特性阻抗	(157)
15. RECOMMENDATION AND REFERENCE TABLE OF RIGID ELLIPTICAL WAVEGUIDE DATA	(167)
16. PROPERTIES OF RECTANGULAR AND TROUGH LINE WITH CIRCULAR INNER CONDUCTOR	(170)
17. 两无限长共轴圆锥体间的特性阻抗	(180)
18. CONTRIBUTIONS TO THE THEORY OF NON-IDEAL WAVEGUIDES	(183)
19. 具有矩形内导体,圆柱外导体的同轴线的特性阻抗	(188)
20. A Critical Study of the Coaxial Transmission Line Utilizing Conductors of Both Circular and Square Cross Section	(195)
21. SOLUTIONS OF SOME TRANSMISSION LINES	(202)

22. 未屏蔽平板线的进一步研究	(206)
23. 脊峰形同轴波导的工作特性	(210)
第三部分 含不均匀介质的波导传输理论的研究	(212)
1. Electromagnetic Wave Propagating in Uniform Waveguides Containing Inhomogeneous Dielectric	(212)
2. Mode theory of uniform waveguides filled with dielectric inhomogeneous along one direction only	(221)
第四部分 非圆介质光波导的平均取值法	(227)
1. APPROXIMATE DISPERSION CURVES OF SOME NONCIRCULAR DIELECTRIC OPTICAL WAVEGUIDES	(227)
2. Low-Frequency Scattering of Dielectric Cylinders	(231)
3. LOW-FREQUENCY SCATTERING BY POLYGONAL CYLINDERS	(237)
4. 有限长正方形柱导体电容值的一个新的计算方法	(252)
第五部分 波导不连续性的等效电路	(255)
1. THE PROBLEM OF A CONDUCTING SPHERE RESTING ON AN EARTHED PLANE IN A UNIFORM PERPENDICULAR FIELD AND ITS APPLICATIONS	(255)
2. 矩形波导一个不连续性的等效电路	(258)
3. THE COMPUTATION ON AND THE ANALYSIS OF COAXIAL BANDPASS FILTERS	(275)
第六部分 小孔耦合理论的应用	(292)
1. COUPLING BETWEEN A RECTANGULAR WAVEGUIDE AND A CIRCULAR WAVEGUIDE OR A CYLINDRICAL CAVITY THROUGH A SMALL HOLE	(292)
2. 格林函数在计算部分电容中的应用	(301)
第七部分 综合研究	(313)
1. MICROWAVE RESEARCH IN CHINA	(313)
2. 任意截面波导中 TE 波的截止波长的一个模拟测量方法	(317)
3. 平面上无限长开槽衍射问题的一个新解法	(324)
4. 调频讯号的一些特性	(327)
5. 贝塞尔函数的近似计算在调频制中的应用	(338)
6. Measurement and Calibration of a Universal Six-Port Network Analyzer	(345)

第一部分 一腔多模微波电路理论与应用

作者从谐振频率的基本公式出发,发现圆柱谐振腔中存在着二、三、四及五个简并模,故一个腔可当二、三、四个及五个腔用。这个发现连同作者第一次建立的一腔五模微波滤波器发表在美国应用物理杂志 1951 年八期首页,引起了广大同行的极大注意。到六十年代卫星通讯的出现,人们对这种滤波器的重视程度又大为增加,卫星通讯技术杂志第一卷第一期又重提本发明的意义。1984 年作者发表了“一腔双模理论及其在测量纸张湿度中的作用”。根据这个理论研制成的纸张测湿仪在国内被广泛采用。

1. Microwave Filters Employing a Single Cavity Excited in More than One Mode*

WEI-GUAN LIN

Division of Electrical Engineering, University of California, Berkeley, California

(Received October 27, 1950)

A cavity resonator with input and output couplings represents a two-terminal-pair network with an infinite number of natural modes of oscillation. In some cavities of special shape, a number of degenerate modes with identical natural frequencies can be found. In a single cavity, various numbers of these degenerate modes can be coupled together to form a chain of coupled circuits by perturbing the otherwise ideal geometrical configuration of the cavity. The filter behavior is prescribed, and the two-terminal-pair network realizing this is obtained by a process of synthesis.

I. INTRODUCTION

IN a single cavity resonator there are an infinite number of modes. Suggestion on the possibility of utilizing some of them to form a multimode coupled circuit by means of a single cavity have been made¹, with the advantage of saving space, weight, and cost. An experimental mode of a two-mode filter has been described in the literature.¹ This employs two perpendicularly polarized TE₁₁₁ modes to give the equivalence of two tuned circuits of a two-stage coupled circuit. One cavity or one iris is thus saved, but the single cavity is more complex. The full advantages of the principle can be realized only when we can control more than three modes in a single cavity.

The purpose of this report is to carry through the theoretical analysis to investigate the number of modes that is useful for our purpose of deriving a multimode filter.

II. A SINGLE CAVITY EXCITED WITH MORE THAN ONE MODE

1. Number of Possible Useful Modes in a Single Cavity

The interaction between the free oscillations of two tuned circuits depends on the coupling coefficient and on the ratio of their complex resonant frequencies.

The closer the two frequencies are to each other, the less coupling is needed to transfer energy between the two circuits. In the problem of coupling together the various resonant modes in a single cavity resonator, the coefficient of coupling is inherently low, because, in an ideal region of simple geometrical configurations enclosed by perfectly conducting walls, orthogonality exists among the infinite number of modes, small perturbations in the otherwise ideal cavity configuration are introduced, and this perturbation must be small if small perturbation theory is to be applied. Therefore, the modes of a single cavity which could be useful for our purpose of filter circuits must possess the same resonant frequencies or, in other words, should be degenerate modes.

For a rectangular cavity resonator bounded by perfectly conducting walls at $x=0, a; y=0, b; z=0, c$; the resonant wavelength for both the TM and the TE waves is given by

$$\lambda = [(l/2a)^2 + (m/2b)^2 + (n/2c)^2]^{-\frac{1}{2}}, \quad (1)$$

where l, m , and n are the integer indices, one but not two of which may vanish. Moreover, $n=0$ is not allowed for the TE waves.

It can readily be seen that $a=b=c$ gives numerous numbers of degenerate modes with identical natural wavelengths. Because when λ is fixed, given by $2a/N$, $N^2 = l^2 + m^2 + n^2$, and as N is made larger and larger, there exist more and more possible combinations of

* J. Appl. Phys., August, 1951

¹ G. L. Ragan, *Microwave Transmission Circuits* (McGraw-Hill Book Company, Inc., New York, 1948), M. I. T. Radiation Laboratory Series, Vol. 9, PP. 673-677.

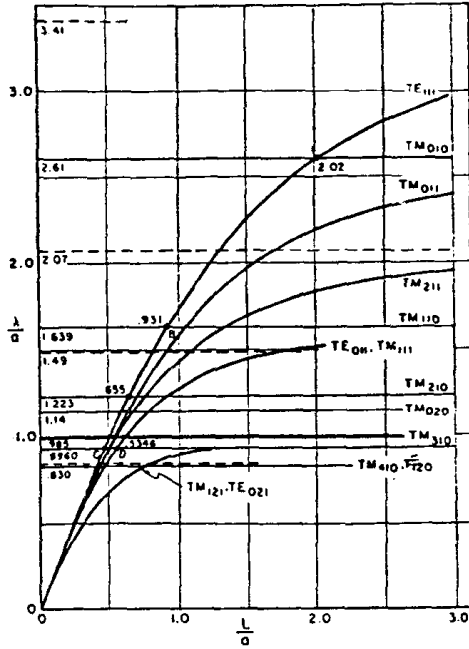


FIG. 1. Natural wavelengths of a circular cavity.

integers l , m , and n . For a given set of l , m , and n , there are six distinct permutations; this together with the fact that Eq. (1) characterizes both TE and TM waves makes the number of degenerate modes twelve when $n=0$, and ten when $n \neq 0$ (TE_{lm0} and TE_{mlo} are not allowed). However, we should observe that, for a given λ , the linear dimension a is larger the higher the order of degeneracy is; therefore, the number of modes that is practical is still limited.

For the next case of a cylindrical cavity bounded by the cylindrical surface $r=a$ and planes $z=0$ and $z=c$, the natural wavelength is given by

$$\frac{\lambda}{a} = \frac{2\pi}{[X_{lm}^2 + n^2\pi^2/(c/a)^2]^{1/2}}, \quad (2)$$

where n is an integer, and X_{lm} is the m th root either of $J_l(X)$ for the TM waves, or of $J_l'(X)$ for the TE waves. Here $n=0$ is not allowed for the TE waves.

In Fig. 1, λ/a (of Eq. (2)) is plotted as a function of the ratio l/a for some of the lower modes, $n=1$. It is readily seen that any mode that is not axially symmetric is twofold degenerate, i.e., two identical modes with perpendicular polarizations. At A, $\lambda/a=2.02$; the two TE_{111} 's and the TM_{010} give another case of degeneracy. At points such as B and C, we have four modes of the same λ/a -ratios, i.e., two TE_{111} (even and odd) and two TM_{110} (even and odd) at B, and two TE_{111} and two TM_{120} at C. At point D, we have five modes: one circularly symmetrical TE_{011} mode, two TM_{111} modes with perpendicular polarizations, and two TM_{120} modes also with perpendicular polarizations. As we go further down in the graph, we will find many points where there are five modes of the same λ/a -ratio (wherever the functions $J_{0m}(X)$ and $J_{lm}'(X)$ have the same zero); however, no point can be found with more than five modes, for $n=1$. When n is allowed to take on values greater than one, the number of degenerate modes can be increased. For instance, at the point where the λ/a curves of the TE_{0mn} and the $TE_{0m'n'}$

meet, together with their dual TM modes, we have six degenerate modes. At this point, however, the size of the cavity is considerably increased, as can be seen by letting $m=2$, $n=1$, $m'=1$, and $n'=2$. Thus, we shall confine our investigation to cases where $n=1$.

For a spherical cavity, from

$$\left(\frac{\pi}{2r}\right)^{1/2} J_{n+1/2}(kr) P_n^m(\cos\theta) \begin{matrix} \cos m\phi \\ \sin m\phi \end{matrix},$$

the basic wave solution for such a cavity, and from the fundamental boundary condition, we obtain the characteristic values of both the magnetic and the electric modes, respectively, with the following equations:

$$j_n(kr) = (\pi/2r)^{1/2} J_{n+1/2}(kr) = 0, \quad (3)$$

$$[kr j_n(kr)]' = 0.$$

These two equations possess distinct roots. Therefore, all the degenerate modes belong to the same type of waves, either magnetic or electric. For each type of wave, subject to condition (3), there are the even and odd modes in the ϕ -variation (except $m=0$). In the θ -variation, there are $n+1$ degenerate modes. Thus, for a particular characteristic number k_a , there may be as many as $2n+1$ degenerate modes.

The circular cavity is actually a limiting case of an elliptical cavity, so that the latter cannot be employed to give more degenerate modes. All other cavities of various geometrical configuration, such as coaxial or biconical cavities, likewise do not give more modes. They are, moreover, difficult to make.

2. A Single Cavity Excited with Two Modes

Let the circular cavity supporting the lowest mode be end-on coupled to two rectangular guides, supporting only the dominant mode, through small irises in the centers of its two end plates. The two broad faces of these guides are, however, 90° to each other. Theoretical and experimental² investigations point out that there exist two resonant modes in the cavity with perpendicular polarization; i.e., the angular variation is $\sin\phi$ for one and $\cos\phi$ for the other, each being in alignment with the exciting mode in the exciting guide. No coupling, then, exists between these two modes, nor any between the input and the output guides in the ideal case free from any irregularity in the cavity.

Coupling will exist between them, however, when the ideal case is disturbed. To find the coefficient of coupling, we start with free oscillations. Assuming that only two modes, a and b , are excited, the field in the cavity is given by

$$\begin{aligned} \vec{H} &= A\vec{H}_a + B\vec{H}_b, \\ \vec{E} &= C\vec{E}_a + D\vec{E}_b, \end{aligned} \quad (4)$$

where

$$a = \int \vec{E} \cdot \vec{E}_a d\tau, \quad C = \int \vec{E}_a \cdot \vec{E} d\tau, \quad \text{etc.,}$$

and \vec{H}_a and \vec{E}_a are normalized functions which have been defined by Slater³ as follows:

² W. W. Balwanz, "The resonant frequency of a cavity-type filter as a function of the size of the coupling iris," NRL Report R-3399, Naval Research Lab, Washington, D. C. (1949).

$$\begin{aligned} \int_V \vec{E}_a \cdot \vec{E}_b dv &= \begin{cases} 1, & a=b \\ 0, & a \neq b \end{cases}, & k_a \vec{E}_a &= \nabla \times \vec{H}_a, \\ \int_V \vec{H}_a \cdot \vec{H}_b dv &= \begin{cases} 1, & a=b \\ 0, & a \neq b \end{cases}, & k_a \vec{H}_a &= \nabla \times \vec{E}_a, \end{aligned} \quad (5)$$

where k_a is the characteristic constant for the particular function.

Now we perturb the cavity boundary by pushing a small portion of the boundary surface into the cavity (by inserting a small screw, for instance). In the small volume between the original surface and the perturbed surface, the final \vec{E} and \vec{H} will be zero. There exists then a surface current, equal to $\vec{n} \times \vec{H}$, corresponding to the discontinuity of \vec{H} . Putting Eqs. (4) into the result of the method of orthogonal functions, Eqs. (III, 42, 43) of Slater's paper,³ we have, over the small perturbation surface, for a time variation of $e^{i\omega t}$,

$$\begin{aligned} (\omega_a^2 - \omega^2)A &= [\omega_a / (\mu_0 \epsilon_0)^{1/2}] \int_{S'} \vec{n} \times \vec{H} \cdot \vec{E}_a da, \\ (\omega_b^2 - \omega^2)B &= [\omega_b / (\mu_0 \epsilon_0)^{1/2}] \int_{S'} \vec{n} \times \vec{H} \cdot \vec{E}_b da. \end{aligned} \quad (6)$$

If the perturbation is small, the perturbed field is very nearly equal to the original field, and we can then substitute the value of \vec{H} from (4). We then write:

$$\begin{aligned} \int_{S'} \vec{n} \times \vec{H} \cdot \vec{E}_a da &= A \int_{S'} \vec{n} \times \vec{H}_a \cdot \vec{E}_a da \\ &+ B \int_{S'} \vec{n} \times \vec{H}_b \cdot \vec{E}_a da. \end{aligned} \quad (7)$$

The integration is carried over the small perturbation surface S' . The integrations on the right can be transformed further by converting surface integrals into volume integrals and by expanding the divergence of the cross product of two vectors,

$$\begin{aligned} [\omega^2 - \omega_a^2(1+m)]A - [\omega^2 p - \omega_a \omega_b q]B &= 0, \\ -[\omega_b^2 p - \omega_a \omega_b q]A + [\omega^2 - \omega_b^2(1+n)]B &= 0, \end{aligned} \quad (8)$$

where we have written

$$\begin{aligned} m &= \int_{V'} (H_a^2 - E_a^2) dv, & n &= \int_{V'} (H_b^2 - E_b^2) dv, \\ p &= \int_{V'} \vec{H}_a \cdot \vec{H}_b dv, & q &= \int_{V'} \vec{E}_a \cdot \vec{E}_b dv. \end{aligned}$$

When the two modes a and b are identical, $\omega_a = \omega_b = \omega_0$, and if the coupling screw possesses such symmetries that $m = n$, we have, from (8),

$$\begin{aligned} \omega^2 &= \omega_0^2 [1 + m \pm (p - q)] \\ &= \omega_0^2 (1 + m) \{ 1 \pm [(p - q)/(1 + m)] \}, \\ \omega &\cong \omega_0 (1 + m)^{1/2} \{ 1 \pm [(p - q)/2(1 + m)] \}, \end{aligned} \quad (9)$$

when $p, q, m \ll 1$.

Comparing this result with the conventional coupled

circuits tuned to the same resonant frequency, it is seen that the modes in the cavity have a coefficient of coupling

$$k = (p - q)/(1 + m). \quad (10)$$

The perturbation of the surface changes also the resonant frequency of each mode slightly.

Thus, we see that the input or the output guide together with its excited mode is represented by one-half of the circuit of Fig. 2(a). They would be independent of each other, were there no perturbation in the cavity proper. The coefficient of coupling M exists because of the insertion of a coupling screw, producing the required perturbation. This is then the equivalent circuit of our filter, b_1 and b_2 being the discontinuity susceptances between the input and output guides to the cavity, respectively. Figure 2(b) is ob-

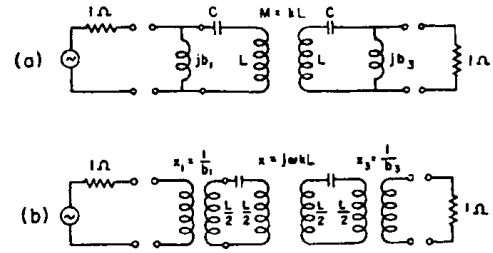


FIG. 2. The equivalent circuit of a single cavity excited with 2 modes.

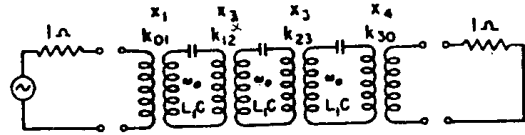


FIG. 3. The equivalent circuit of a single cavity excited with 3 modes.

tained from Fig. 2(a) by transforming the shunt coil into a loss-free transformer and by neglecting quantities of the order of $1/b_1$ in the series loops.

3. A Single Cavity Excited with Three Modes

At point A of Fig. 1 there are two TE_{111} modes and one TM_{010} mode with identical $\lambda/a = 2.02$. Now, if the circular cavity of the preceding section (Sec. II, 2, Eq. (2)) is so scaled that the ratio λ/a is just 2.02, and if two coupling screws are inserted at each end of the cylindrical guide wall, each in line with the maximum electrical intensity of the input and the output rectangular guides, then in the round cavity there will be two orthogonal TE_{111} modes, each corresponding to one of the input and output guides, and one TM_{010} mode. There is no coupling between the TE_{10} mode in the rectangular guide and the TM_{010} mode in the round guide, because at the central hole, the tangential magnetic field of the latter mode vanishes, and former mode has no E_z . Also, there is no direct coupling between the two orthogonal TE_{111} modes when the coupling screws are so located and are 90° apart. Any coupling between the input and output circuits is through one TE_{111} to TM_{010} , and TM_{010} to the other TE_{111} . We thus establish an over-all system of a chain

³ J. C. Slater, Revs. Modern Phys. Vol. 18, 441 (1946).

of three resonant circuits, represented by Fig. 3, where

$$\begin{aligned} k_{12} &= (p_{12} - q_{12}) / (1 + m_{11}), \\ k_{23} &= (p_{23} - q_{23}) / (1 + m_{22}), \end{aligned} \quad (11)$$

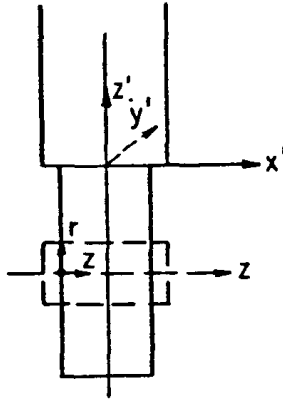


FIG. 4. Coupling between rectangular guides and the round cavity for a 4-mode filter.

TABLE I. Nonvanishing field components for the 4-mode cavity (point B of Fig. 1).

MODE POINT	INPUT TE ₁₀	(1) (0) TE ₁₁₁	(2) (0) TM ₁₁₀	(3) (0) TM ₁₁₀	(4) (0) TE ₁₁₁	OUTPUT TE ₁₀
(0, 0°, 0)	H _{x'}	H _z	H _φ			
	k ₀₁ ≠ 0					
(0, 90°, 0)				H _φ	H _z	H _{x'}
					k ₄₀ ≠ 0	
(0, 0°, 0)		H _r	H _r	H _φ	H _φ	
		k ₁₂ ≠ 0		k ₃₄ ≠ 0		
(0, 90°, 0)		H _φ	H _φ	H _r	H _r	
		k ₁₂ ≠ 0		k ₁₄ ≠ 0		
(0, 45°, 0)		H _z	H _φ	H _φ	H _z	
		k ₁₄ ≠ 0	k ₂₃ ≠ 0			

with

$$\begin{aligned} m_{ii} &= \int_{\text{SCREWS}} (H_i^2 - E_i^2) dv, \\ P_{ij} &= \int_{\text{SCREWS}} \bar{H}_i \cdot \bar{H}_j dv, \\ q_{ij} &= \int_{\text{SCREWS}} \bar{E}_i \cdot \bar{E}_j dv, \end{aligned} \quad (12)$$

where \bar{E}_i and \bar{H}_i are the normalized field intensities evaluated at the tuning screw.

4. A Single Cavity Excited with Four and Five Modes

To correspond to B (also C) of Fig. 1, we take Fig. 4, where two rectangular guides are coupled to the cavity through two holes 90° apart on the cylindrical wall. The broad face of the former is parallel to the longitudinal axis of the latter. The two guides are perpendicular themselves. In Table I, we tabulate the nonvanishing field components at some favorable points where we are going to introduce the perturbations to effect the couplings for the modes of point B. The vari-

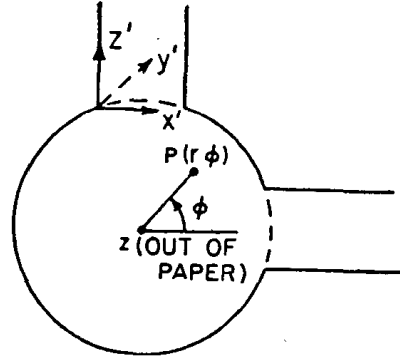


FIG. 5. Coupling between rectangular guides and the round cavity for a 5-mode filter.

ous coefficients of coupling are given by

$$k_{ij} = (p_{ij} - q_{ij}) / (1 + m_{ii}) \quad (13)$$

where m_{ii} , p_{ij} , and q_{ij} are given by (12).

The case of point D in Fig. 1 is realized by the arrangement shown in Fig. 5. The transverse magnetic field in the rectangular guide is aligned with the azimuthal component of the magnetic field of the TM_{120} mode in the round cavity. In Table II, the nonvanishing field components of the various modes at some preferable points are again given, and the coupling coefficients among the modes are examined.

TABLE II. Nonvanishing field components for the 5-mode cavity (point D of Fig. 1). ($J_1(x_{11}) = J_1(3.832) = 0$; $J_1(x_{12}) = J_1(7.0156) = 0$.)

MODE POINT	INPUT TE ₁₀	(1) (0) TM ₁₂₀	(2) (0) TM ₁₁₁	(3) (0) TE ₀₁₁	(4) (0) TM ₁₁₁	(5) (0) TM ₁₂₀	OUTPUT TE ₁₀
(0, 0°, 0)	H _{x'}	H _φ	E _r	H _z			
	k ₁₀ ≠ 0						
(0, 90°, 0)				H _z	E _r	H _φ	H _x
						k ₅₀ ≠ 0	
(0, 0°, 0)		H _φ	H _φ	H _z			
		k ₁₂ ≠ 0					
(0, 90°, 0)				H _z	H _φ	H _φ	
					k ₄₅ ≠ 0		
(0, 0°, 90°)		H _φ	H _r	H _r			
			k ₂₃ ≠ 0				
(0, 0°, 0)				H _φ	H _r	H _r	
					k ₄₅ ≠ 0		

From Tables I and II, the exact equivalent circuits of the 4-mode and the 5-mode cavity are derived, respectively, and they are represented by Fig. 6 and Fig. 7.

5. Prescription of the Filter Characteristics

The equivalent circuits of a single cavity excited with various numbers of modes are all band-pass filters whose characteristics can be obtained from a prototype low-pass with a cut-off frequency of one radian per second, according to the principle of frequency normalization. The prototype structure of Fig. 8 is transformed into a chain of coupled circuits such as the one

of Fig. 7 when the frequency transformation,

$$x = (\omega_0/W)[(\omega/\omega_c) - (\omega_0/\omega)] \quad (14)$$

is made, where ω_0 is the resonant frequency and W the bandwidth. When we identify Fig. 7 with Fig. 8, we

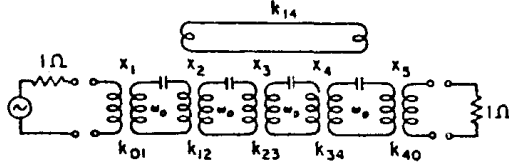


FIG. 6. The exact equivalent circuit of a 4-mode filter.

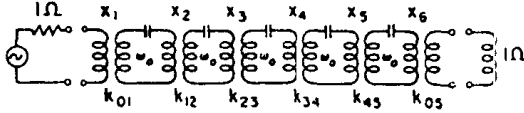


FIG. 7. The exact equivalent circuit of a 5-mode filter.

have

$$\begin{aligned} X_1^2 &= (L/C_1)W, \\ X_{2k}^2 &= LW^2/L_{2k}C_{2k-1} = X_1^2 C_1^2/L_{2k}C_{2k-1}, \\ X_{2k+1}^2 &= LW^2/L_{2k}C_{2k+1} = X_1^2 C_1^2/L_{2k}C_{2k+1}, \\ X_{n+1}^2 &= WLR/L_n = X_1^2 C_1 R/L_n \quad \text{for } n \text{ even}, \\ X_{n+1}^2 &= WL/RC_n = X_1^2 C_1/RC_n \quad \text{for } n \text{ odd}. \end{aligned} \quad (15)$$

The insertion loss characteristic of Fig. 8 can now be prescribed; let

$$L_n = 10 \log(P_0/P_L)_n = 10 \log[1 + h^2 T_n^2(x)], \quad (16)$$

where $T_n(x)$ is the Tchebyshev polynomial of n th degree, and h^2 is an arbitrary constant which controls the tolerance in the pass band. When h is small, the maximum insertion loss in the pass band is

$$L_{\max} = 10 \log(1 + h^2) = 4.23h^2, \quad \text{for } h^2 \ll 1.$$

a. Two- and Three-Mode Filters

The actual values of the circuit elements of Fig. 8, for the cases of $n=2$ and $n=3$, can be solved by the elementary circuit theory. Thus (refer to Fig. 2(b)) symmetry consideration gives $X_1^2 = X_2^2$, and, consequently,

$$\begin{aligned} R &= L_2/C_1, \\ h^2 &= (1-R)^2/4R, \\ C_1^2 &= 2(1-R)/R. \end{aligned} \quad (17)$$

The choice of elements C_1 and R is controlled by the pass-band tolerance h^2 .

For the case of $n=3$, symmetry requires $X_1^2 = X_3^2$, or $R = C_1/C_3$ and $C_1 = C_3$, or $R=1$. The expression for

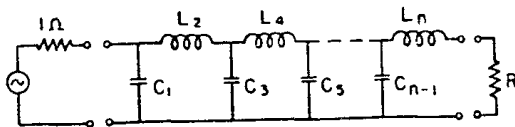


FIG. 8. A prototype low-pass filter.

P_0/P_L is

$$P_0/P_L = 1 + \frac{1}{4}[L_2 C_1^2 x^2 - (2C_1 - L_2)x]^2. \quad (18)$$

Identifying the coefficients of the quantity inside the bracket with those of $T_3(x)$, we have

$$\begin{aligned} L_2 C_1^2 &= 4, \\ 2C_1 - L_2 &= 3, \end{aligned}$$

one solution of which is (the other two roots form a complex pair)

$$\begin{aligned} C_1 &= C_3 = 2, \\ L_2 &= 1. \end{aligned} \quad (19)$$

To treat the cases of $n=4$ and 5, we define the power insertion loss P_0/P_L as

$$L = P_0/P_L = |\rho(j\omega)|^2, \quad (20)$$

where ρ is the voltage insertion loss ratio, i.e., the ratio between the voltages across the load resistance with the network interposed and with an ideal transformer inserted and adjusted for a match maximum power transfer; and the reflection coefficient is

$$\Gamma(p) = [1 - Z(p)]/[1 + Z(p)], \quad p = \sigma + j\omega, \quad (21)$$

the complex frequency,

where $Z(p)$ is the input impedance of the terminated network, Γ being related to the power insertion loss ratio by the following equation:

$$L = \frac{P_0}{P_L} = \frac{1}{1 - |\Gamma(j\omega)|^2},$$

or

$$|\Gamma(j\omega)|^2 = \frac{1}{(1 + 1/P_0/P_L)}; \quad (22)$$

and from (21),

$$Z(p) = [1 + \Gamma(p)]/[1 - \Gamma(p)]. \quad (23)$$

Since $Z(p)$ is positive real, $|\Gamma(p)| \leq 1$ for $\text{Re}(p) \geq 0$. Also, $\Gamma(p)$ is analytic for $\text{Re}(p) \geq 0$, because $1 + Z(p)$ cannot vanish on the imaginary axis if $Z(p)$ is real positive. The poles of $\Gamma(p)$ and zeros of $\rho(p)$ are, therefore, confined to the left-half p -plane; thus, for a given $L(\omega)$, from (22), the poles of $\Gamma(p)$ and consequently $L(p)$ itself can be found if $L(\omega)$ has no finite poles. Similarly, $\rho(p)$ can be found from (20). Then $Z(p)$ is obtained from (23). The network realizing this $Z(p)$, and thus realizing the prescribed characteristic, is to be obtained by a process of synthesis.

For the four- and five-mode filters, let

$$\begin{aligned} L_4 &= 1 + \frac{1}{4}T_4^2(x) = 1 + \frac{1}{4}(8x^4 - 8x^2 + 1), \\ L_5 &= 1 + \frac{1}{4}T_5^2(x) = 1 + \frac{1}{4}(16x^5 - 20x^3 + 5x), \end{aligned} \quad (24)$$

so that the pass-band tolerance is about 1 db. By locating the roots of $\rho(p)$ from (24) and those of $Z(p)$ from (22), we have

$$\rho_4(p) = 4(p^4 + 0.96p^3 + 1.46p^2 + 0.75p + 0.28), \quad (25)$$

$$\rho_5(p) = 8(p^5 + 0.941p^4 + 1.696p^3 + 0.983p^2 + 0.585p + 1.25),$$

$$\Gamma_4 = -\frac{p^4 + p^2 + 0.125}{(p^4 + 1.46p^2 + 0.28) + (0.96p^3 + 0.75p)}, \quad (26)$$

$$\Gamma_5 = -\frac{p^5 + 1.25p^3 + 0.312p}{(0.948p^4 + 0.96p^2 + 0.125) + (p^5 + 1.701p^3 + 0.5897p)}.$$

To realize the networks giving these two reflection coefficients, we find that

$$\begin{aligned} 1/Z_4 &= 2.083p + 1/1.068p + 1/2.83p \\ &\quad + 1/2.83p + 1/0.785p + 0.383, \\ 1/Z_5 &= 2.1186p + 1/1.0964p + 1/2.969p \\ &\quad + 1/2.969p + 1/2.1186p + 1, \end{aligned} \quad (27)$$

respectively, for the cases of $n=4$ and $n=5$. The prototype structures in Fig. 9 correspond to Eqs. (27).

The dissipation is taken into account by assuming that the complex frequency p possesses a small but constant real part δ ; and the dissipative insertion losses are as follows, neglecting terms involving δ of higher power than the third, $h=1$ for $n=2$ and $h=\frac{1}{2}$ for all

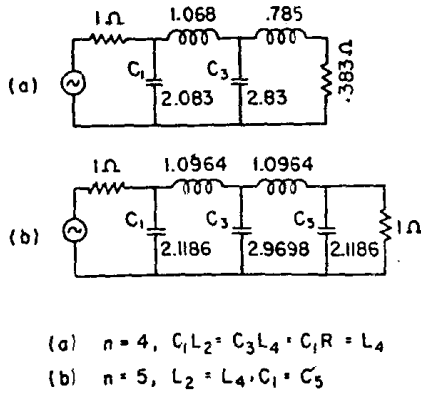


FIG. 9. Prototype structures for the 4- and 5-mode filter.

the others,

$$\begin{aligned} L_2' &= 4\{(\delta^2 + 0.644\delta + 0.707 - x^2)^2 + (0.644 + 2\delta)x^2\}, \\ L_3' &= 4\{[\delta^2 + \delta^2 + 1.25\delta + 0.5 - (3\delta + 1)x^2]^2 \\ &\quad + x^2[3\delta^2 + 2\delta + 1.25 - x^2]^2\}, \end{aligned} \quad (28)$$

$$\begin{aligned} L_4' &= 64\{[(5\delta + 0.944)x^4 - (10\delta^2 + 5.66\delta^2 + 5.09\delta \\ &\quad + 0.983)x^2 + (1.696\delta^2 + 0.983\delta^2 + 0.585\delta \\ &\quad + 1.25)]^2 + x^2[(4\delta + 0.96)x^2 - (2.88\delta^2 \\ &\quad + 0.292\delta + 0.75)]^2\}, \end{aligned}$$

$$\begin{aligned} L_5' &= 64\{[(5\delta + 0.944)x^4 - (10\delta^2 + 5.66\delta^2 + 5.09\delta \\ &\quad + 0.983)x^2 + (1.096\delta^2 + 0.983\delta^2 + 0.585\delta \\ &\quad + 0.125)]^2 + x^2[x^4 - (10\delta^2 + 3.78\delta + 1.69)x^2 \\ &\quad + (3.77\delta^2 + 5.09\delta^2 + 1.966\delta + 0.585)]^2\}, \\ \delta &= R/L = (\omega_0/w)1/Q. \end{aligned} \quad (29)$$

6. Coupling Elements of a Cavity Excited with Multimodes

Equations (14), (17), (19), and (27) give complete design data for our cavity filter. To obtain the actual

coupling design, the value of L for each cavity must be evaluated explicitly. Let a cavity be formed by closing

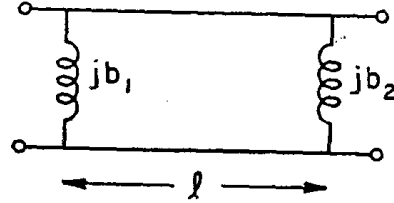


FIG. 10. The transmission line equivalent of a single cavity in wave guides.

a piece of wave guide by two end plates on which there are coupling devices, such as irises, etc. Then we have the circuit of Fig. 10 with open circuit admittances B_{11} and B_{22} as follows:

$$\begin{aligned} B_{11} &= \left(\frac{\epsilon}{\mu}\right)^{\frac{1}{2}} \left[1 - \left(\frac{\omega_c}{\omega}\right)^2\right]^{\frac{1}{2}} \\ &\quad \times \left\{ b_2 + \tan\left[\frac{l}{c}(\omega^2 - \omega_c^2)^{\frac{1}{2}}\right] \right. \\ &\quad \times \left. b_1 + \frac{1 - b_2 \tan\left[\frac{l}{c}(\omega^2 - \omega_c^2)^{\frac{1}{2}}\right]}{1 - b_1 \tan\left[\frac{l}{c}(\omega^2 - \omega_c^2)^{\frac{1}{2}}\right]} \right\}, \\ B_{22} &= \left(\frac{\epsilon}{\mu}\right)^{\frac{1}{2}} \left[1 - \left(\frac{\omega_c}{\omega}\right)^2\right]^{\frac{1}{2}} \\ &\quad \times \left\{ b_1 + \tan\left[\frac{l}{c}(\omega^2 - \omega_c^2)^{\frac{1}{2}}\right] \right. \\ &\quad \times \left. b_2 + \frac{1 - b_1 \tan\left[\frac{l}{c}(\omega^2 - \omega_c^2)^{\frac{1}{2}}\right]}{1 - b_2 \tan\left[\frac{l}{c}(\omega^2 - \omega_c^2)^{\frac{1}{2}}\right]} \right\}. \end{aligned} \quad (30)$$

At $\omega = \omega_0$, the resonant frequency, both B_{11} and B_{22} vanish. The proper length, l , of the cavity can be found from

$$\tan\left[\frac{l}{c}(\omega^2 - \omega_c^2)^{\frac{1}{2}}\right] = \frac{b_1 + b_2}{b_1 b_2 - 1} \approx \frac{1}{b_1} \quad \text{for } b_2 \gg b_1 \gg 1, \quad (31)$$

and the slopes of B_{11} and B_{22} at $\omega = \omega_0$, their common zero, are given by

$$\begin{aligned} dB_{11}/d\omega|_{\omega=\omega_0} &= n\pi[(b_1^2 - 1)/(\omega_0^2 - \omega_c^2)^{\frac{1}{2}}](\epsilon/\mu)^{\frac{1}{2}}, \\ dB_{22}/d\omega|_{\omega=\omega_0} &= dB_{11}/d\omega|_{\omega=\omega_0}, \end{aligned} \quad (32)$$

for large values of b_1 and b_2 .

Now we know that, for a cavity coupled with two wave guides,^{3,4}

$$L_1/\omega_0^2 M_1 = \frac{1}{2} dB_{11}/d\omega|_{\omega=\omega_0}$$

or

$$\frac{L_1}{X_1^2} = \frac{1}{2} n\pi \left(\frac{\epsilon}{\mu}\right)^{\frac{1}{2}} \frac{b_1^2}{\omega_0(1 - \omega_c^2/\omega_0^2)^{\frac{1}{2}}}. \quad (33)$$

Substituting the value for X_1^2 from (15), we have

$$b_1^2 = (2C_1/n\pi)(\omega_0/\omega)(1-\omega_c^2/\omega^2)(\mu/\epsilon)^{1/2}(L_1/L) \times \{1-\omega_c^2/\omega_0^2\}^{-1/2}. \quad (34)$$

But L is already normalized, i.e.,

$$L = L_1/(\mu/\epsilon)^{1/2}[1-(\omega_c/\omega)^2]^{1/2}. \quad (35)$$

Therefore, the end result is

$$|b_1| = \left\{ \frac{2C_1 \omega_0}{n\pi w} \left[1 - \left(\frac{\omega_c}{\omega_0} \right)^2 \right] \right\}^{1/2} \frac{\lambda}{\lambda_g} \left\{ \frac{2C_1 \omega_0}{n\pi w} \right\}^{1/2}. \quad (36)$$

We see that this value of b_1 is normalized with respect to the guide impedance that forms the cavity proper. However, for subsequent work we need the value of $|b_1|$ normalized with respect to the input and output guides, which for symmetrical operations are identical; therefore, we should write, in that case,

$$|b_1| = [\lambda_g^{(a)}\lambda/(\lambda_g^{(c)})^2]^{1/2} \{ (2C_1/n\pi)(\omega_0/w) \}^{1/2}, \quad (37)$$

where $\lambda_g^{(a)}$ is the guide wavelength in the coupled guides, and $\lambda_g^{(c)}$ is that in the cavity proper. This change of scale is justified once we assume the pass band is small so that we can neglect the frequency sensitivity of the coupling susceptances.

From Eqs. (15) we find that

$$\begin{aligned} k &= (W/\omega_0)[RC_1^2]^{-1/2} && \text{for 2-mode cavity} \\ k_{12} &= (W/\omega_0)[C_1L_2]^{-1/2} && \text{for 3-mode cavity} \\ k_{23} &= (W/\omega_0)[L_2C_3]^{-1/2} && \\ k_{12} &= k_{34} = (W/\omega_0)[L_2C_1]^{-1/2} && \text{for 4-mode cavity} \\ k_{23} &= (W/\omega_0)[L_2C_3]^{-1/2} && \\ k_{12} &= k_{45} = (W/\omega_0)[L_2C_1]^{-1/2} && \text{for 5-mode cavity.} \\ k_{23} &= k_{34} = (W/\omega_0)[L_2C_3]^{-1/2} && \end{aligned} \quad (38)$$

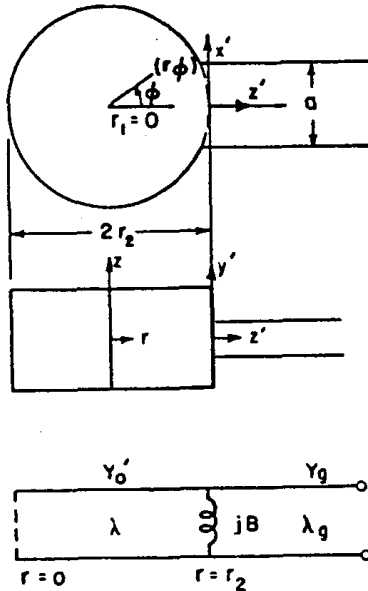


FIG. 11. Equivalent circuit of the coupling between a radial and a uniform transmission line.

7. Small Hole Coupling between Rectangular Guide and Circular Guide or Cavity

In our filters we use rectangular guides for the input and output lines, coupled to the circular cylindrical cavity by inductive irises either on the end-plates or on the cylindrical wall of the latter. Now we will give the discontinuity susceptance to be added to the transmission line circuit. We will assume that the coupling holes are small so that the field in the hole is constant and that the effect of the hole can be replaced by magnetic and electrical dipoles by following Bethe's line of reasoning in his studies⁵ of small holes in an electromagnetic field.

a. End-On Coupling between Rectangular and Circular Guides

Let a wave be incident from the rectangular guide. In the circular guide there will be a transmitted wave through the hole, and a reflected wave is also set up in the rectangular guide. The n th normal mode H - and E -vectors in the guides are normalized:

$$\int_S |\vec{H}_{1,n}|^2 dS = 1, \quad (39)$$

$$\int_S |\vec{E}_{1,n}|^2 dS = Z_{0n}^2, \quad (40)$$

where $Z_{0n} = (\mu/\epsilon)^{1/2}(\lambda_g/\lambda)$ is the wave impedance for the mode which has been taken as a TF wave.

In the rectangular guide we have an incident wave and a reflected wave; in the circular guide we have a single transmitted wave. We then apply Lorentz's reciprocal theorem to the circular guide. In the hole the field is taken as the sum of the fields on both sides of the hole. The magnitude of the transmission coefficient is found,

$$T = 2[1 - (H_{at}/\vec{H}_{at} \cdot \vec{H}_{bt}) + j(-\lambda_g^{(b)}/2\pi \vec{H}_{at} \cdot \vec{H}_{bt})]^{-1}. \quad (41)$$

For small holes the discontinuity susceptance is large; thus, the normalized susceptance is given by

$$b = -(\lambda^{(b)}/2\pi M)(1/\vec{H}_{at} \cdot \vec{H}_{bt}) = 0.467[\lambda_g^{(b)}(\pi R^2 ab)^{1/2}/d^2], \quad (42)$$

where $M = 4/3(\frac{1}{2}d)^3$, and d = diameter of the hole. The field components H_{at} , etc., are defined by (40); quantities with subscript a refer to those in the transmitting rectangular guide, those with subscript b , to the receiving circular guide. The former has a width a and height b , while the latter has a radius R .

b. Coupling between a TE_{10} Mode in a Rectangular Wave Guide and a TM_{120} Mode in a Circular Cavity through a Circular Hole in the Side Wall of the Circular Cavity

Let the narrow side of the rectangular guide be in the direction of the longitudinal axis of the cavity, as shown in Fig. 11. In the rectangular guide there are three field components, H_z' , E_y' , and H_x' , which will excite the H_z , E_z , and H_r , respectively, in the circular cavity. We will consider the cavity as a radial trans-

⁴ S. A. Schelkunoff, Proc. Inst. Radio Engrs. 32, 83 (1944).

⁵ H. A. Bethe, Phys. Rev. 66, 66-63 (1944).

mission line supporting a TM_{10} mode alone, coupled through an inductive admittance to another uniform line supporting the dominant TE_{10} mode. In Fig. 11 we show the coordinates of the coupled system and the equivalent circuit. Energy is considered to be originated in the radial line, propagating through the coupling element to the uniform line.

Now the radius of curvature of the cavity wall is large compared with the linear dimension of the coupling hole, because we are handling only small holes compared with the wavelength, so the field distribution inside the cavity in the neighborhood of the side wall is the same as that in a rectangular guide of width $a' = \pi r_2$ and height $b' = l$. So, for the first approximation, we can treat our present small hole as one that couples together two rectangular wave guides of different transverse dimensions, and the result given by (42) is valid here;

$$b = -(3\lambda_0/d^2)(ab^2l/4\pi)^{1/2} \quad (43)$$

III. APPLICATION TO FILTER DESIGN

Before taking up sample designs, we will review the assumptions we have made or implied and discuss their justifications. There are four main assumptions: (a) the isolation of the coupling discontinuity or iris; (b) the perfectly circular cavity surface; (c) parallel end plates perpendicular to the longitudinal axis of the cavity; and finally (d) small perturbations, i.e., small coupling holes ($d/\lambda \ll 1$) and small screws.

1. Isolation of Discontinuities

In the first case of our problem in which a round wave guide of $\frac{1}{2}\lambda_0$ in length is closed at both ends, the field intensities at one end plate of the higher mode generated at the other are being attenuated by a factor $\exp[-\alpha\lambda_0/2]$ with

$$\frac{1}{2}\alpha\lambda_0 = \pi[(\lambda_c/\lambda_c')^2(\lambda/\lambda_c)^2 - 1]^{1/2} / [1 - (\lambda/\lambda_c)^2]^{1/2}, \quad (44)$$

where $\lambda_c' = (2\pi/x_{mn})a$ is the cut-off wavelength of the high order mode.

For good isolation of the discontinuities at the two end plates, the value of (λ/λ_c) , Eq. (44), should approach unity; i.e., the cavity is operated near the cut-off condition. However, under this operating condition, the Q -value of the cavity is very low. On the other hand, poor isolation of the irises on the end plates introduces the undesirable direct coupling and consequently decreases the attenuation in the stop-band. Hence, appropriate compromise must be made in choosing the operating condition.

In our experimental model of the 2-mode filter, we will so choose the diameter of the cavity that the Q -value is nearly maximum. The attenuation constant for the first higher order mode, TE_{01} , is estimated to be 5, which is considered as satisfactory for good isolation of the two discontinuities.

In both cases of the 3- and 5-mode filters, the dimensions are fixed for the coexistence of the degenerate modes. For the 3-mode case, the value of (44) is slightly less than 5. For the 5-mode filter, if we follow the line of reasoning postulated in Eq. (7), we have then a case of two discontinuities spaced by a distance $\frac{1}{2}\pi a$ in a rectangular wave guide of height $b=l$. Therefore, the ratio of the distance between the two discontinuities to the height of the guide is about 3, giving a value of the attenuation constant, Eq. (44), considerably larger than 5.

2. Ellipticity of the Cavity Wall

When the circular cavity possesses a slight ellipticity, the even and the odd modes will both suffer changes in natural wavelength, but by different amount.^{6,7} To consider the allowable amount of change of the natural wavelengths of the various modes, we recall that, for small detuning, the detuning causes the relative transmission to decrease, and the effective coefficient of coupling to increase to the value given by

$$k_{eff} = [k'^2 + (\Delta/f_0)^2]^{1/2}, \quad (45)$$

where k' is the actual coefficient of coupling, and Δ is the difference between the resonant frequencies of the tuned circuits. The detuning will also make the attenuation curve of the tuned-circuit filter slightly unsymmetrical when the two tuned circuits do not have the same Q -values.

In order to realize the prescribed behavior of the filter, the effective value k_{eff} in Eq. (45) is set equal to the desired value of k for exact tuning. It is then necessary that

$$\Delta/f_0 < k \quad (46)$$

so that k_{eff} will not be greater than k . Equation (46), therefore, serves as the criterion of the amount of detuning and consequently the percentage of ellipticity allowable. Investigations into the actual modes employed bring out the fact that the ellipticity resulting from any reasonable manufacturing deviation in a cavity intended to be circular will not have serious effects on the behavior of the filter.

3. Parallel End Plates Perpendicular to the Cavity Axis

The deviation of the two end plates of the cavity from perpendicularity with the axis introduces again the frequency shift (and thus detuning among the modes) and the undesirable direct coupling among the modes.

Let the two end plates be given by

$$\begin{aligned} z &= d_1 + \alpha_1 x + \beta_1 y, \\ z &= d_2 + l + \alpha_2 x + \beta_2 y, \end{aligned} \quad (47)$$

where the α 's, β 's, and d 's are small quantities measuring the degree of deviation from the ideal case. When they all vanish, we have the ideal case $z=0$ and $z=l$. To investigate the first effect, we make use of Eq. (9),

$$\Delta f/f = \frac{1}{2} m_{ii} = -\frac{1}{2} \int_{v'} (H_i^2 - E_i^2) dV, \quad (48)$$

$$dV = z dA = [d_1 + (\alpha_1 \cos\phi + \beta_1 \sin\phi) \Gamma] da,$$

where v' denotes the difference volume between the deformed cavity and the original unperturbed cavity; H_i and E_i are the normalized field components, evaluated at the unperturbed boundary enclosed by the difference volume:

$$\begin{aligned} \Delta f/f &= (p^2 \pi^2 / k^2 \Gamma^2) (d_1/l), \\ p &= 0, 1, 2, 3, \dots \quad \text{for } TM_{m,p} \\ p &= 1, 2, 3, \dots \quad \text{for } TE_{m,p}. \end{aligned} \quad (49)$$

⁶ L. J. Chu, J. Appl. Phys. 9, 583-591 (1938).

⁷ L. Brillouin, Elec. Commun. 16, 998 (1938).

Taking the second end plate into account we have

$$\Delta f/f = (p^2 \pi^2 / k^2 l^2) [(d_1 - d_2)/l] \\ = p^2 (\lambda/2l)^2 [(d_1 - d_2)/2]. \quad (50)$$

Now if we take Eq. (2), for a small increment in the length l , we can derive the change in the natural wavelength and arrive at the same Eq. (50). Thus, the control of the tolerance in d_1 and d_2 is actually taken care of, by requiring the adherence to the tolerance of the length of the cavity. In our case of the 5-mode filter, by specifying that the relative detuning between the TM_{120} and the TM_{111} be less than the coefficient of coupling between these two modes, we find that the length of the cavity must be scaled to approximately the last thousandth of an inch.

Tilt adjustments, though not critical in causing frequency shift, nevertheless are important in the spurious coupling between certain modes, namely, between the TE_{0np} and the TM_{inp} modes. To make this point clear, we take Eq. (13) (the factor m_i becoming zero for this case),

$$k_{ij} = \int_{v'} \vec{H}_i \cdot \vec{H}_j dv - \int_{v'} \vec{E}_i \cdot \vec{E}_j dv \\ = (\alpha/\sqrt{2} X_{11}) (\lambda/l) \text{ for } TE_{011} \text{ and } TM_{111}^{(e)} \\ = (\beta/\sqrt{2} X_{11}) (\lambda/l) \text{ for } TE_{011} \text{ and } TM_{111}^{(o)}. \quad (13a)$$

Let the actual tilts at the edge of the end plate at the X and the Y axis be, respectively, l_1 and l_2 . Then $\alpha = l_1/a$ and $\beta = l_2/a$, and Eq. (13a) becomes

$$k = [1/\sqrt{2}(3.832)] (\lambda/a) (l_1/l) \\ \text{between } TE_{011} \text{ and } TM_{111}^{(e)} \\ = [1/\sqrt{2}(3.832)] (\lambda/a) (l_2/l) \\ \text{between } TE_{011} \text{ and } TM_{111}^{(o)}, \quad (51)$$

and the order of magnitude of tolerance in the tilt adjustments again can be estimated.

4. Sizes of Coupling Screws and Irises

In the theoretical analysis of the preceding sections, a simple theory of the unloaded cavity with no discontinuity was first established. Small perturbations were then introduced. The effect of the small perturbation was utilized to set up the filter circuit. One would immediately wonder as to how small the perturbation had to be in order for the field distribution to remain the same as that existing according to the simple theory. Experimental work shows that the sizes of coupling screws are not critical at all. That screws of reasonable size can be employed without any deteriorative effect can be justified from the fact that we deal mainly with sinusoidal and first-order and first-kind Bessel functions, both of which are regular at their zeros and have fairly broad maxima. Further experimental evidence² indicates that an iris diameter as large as approximately three-tenths of wavelength (i.e., the narrow dimension of the usual rectangular wave guide) is suitable for transmission with negligible loss when using the TE_{011} and the TM_{111} modes. Therefore, Bethe's diffraction theory of small holes is believed to be useful at least up to this dimension.

5. The Design Problems

The design problems for the 3-mode filter will be discussed in detail to bring out the important point of frequency correction due to screws and irises, and the modification of the actual dimensions of the cavity to account for them.

First we take one of the two identical TE_{111} 's, in Eq. (31); let

$$l = p(\lambda_g/2) - \epsilon(\lambda_g/2\pi), \quad (52)$$

where ϵ is a small dimensionless number, then we have

$$\epsilon = -1/b_1. \quad (53)$$

When b_1 is negative or when the iris is inductive, l is less than p half-wavelengths. In our existing problem, the cavity is also coupled through a hole to a second rectangular guide whose broad face has been turned 90° with respect to that of the first guide. Therefore, the former guide is called upon to propagate the mode TE_{01} instead of the dominant TE_{10} mode; and therefore, as this second hole introduces only a small perturbation effect, we can then assume $b_2 \gg b_1$. For the same reason, the two holes on the end plates and the two screws produce only perturbation effect to the TM_{010} mode. Thus, for both the TE_{111} and the TM_{010} , the corrected frequency is (there is only one perturbation hole to each of the two TE_{111} modes)

$$\omega_i = \omega_0 [1 + \frac{1}{2}(m_{ii} + C_{ii})] \quad i = 1, 2, \dots, \quad (54)$$

with

$$m_{ii} = \int_{\text{screws}} (H_i^2 - E_i^2) d\tau \approx \sum_{\text{screws}} (H_i^2 - E_i^2) V_{s,i}, \\ c_{ii} = 2 \sum_{\text{holes}} (MH_i^2 - PE_i^2),$$

when the holes and the screws are small, and, consequently, the fields are nearly constant over the holes and the screws. Here \vec{H}_i and \vec{E}_i are the normalized fields to be evaluated at the holes and at the screws; M and P are given by Bethe as $4/3(\frac{1}{2}d)^3$ and $\frac{2}{3}(\frac{1}{2}d)^2$, respectively.

Thus, for either of the two TE_{111} and for the TM_{010} , we have, respectively,

$$m_{11} + C_{11} = (16.8/V) (\lambda/\lambda_g)^2 \{ (V_s/10) + (d^2/16) \}, \\ m_{22} + C_{22} = (1/V) \{ 2V_s - 0.573d^2 \} \\ = 2.5k - (0.0182/R) \{ b \}^4. \quad (55)$$

From these equations we find the relative detuning between the TE_{111} and TM_{010} , recalling that $\lambda = 2.61a$, $\lambda_g = 2l = 4.04a$,

$$2\delta\omega/\omega = (m_{11} + C_{11}) - (m_{22} + C_{22}), \quad (56)$$

$$\delta\omega/\omega = (1/2V) \{ 0.603d^2 - 1.296V_s \}, \\ \delta\omega/\omega = -0.778k + (0.0096/b) \{ R \}, \quad (57)$$

where R is in inches. To correct for this small detuning, we can lengthen the cavity slightly to decrease the resonant frequency of the TE_{111} mode. The change in length does not change that of the TM_{010} mode. If we take $l = \frac{1}{2}\lambda_g$ originally, then we have

$$dl/l = -(\lambda_g/\lambda)^2 (d\omega/\omega) = -2.4(\delta\omega/\omega); \quad (58)$$

and the final length of the cavity is

$$l = \frac{1}{2}\lambda_g [1 + (1/\pi b') + 2.4(\delta\omega/\omega)], \quad (59)$$

where

$$b' = (\lambda_0^{(c)}/\lambda_0^{(s)})b, \\ \delta\omega/\omega = -0.778k + (0.0096/|b|R).$$

For the case of the 5-mode filter, (43) gives the discontinuity susceptance between the TE_{01} in the input or output line and the TM_{120} mode in the cavity.

We next will find the change of the natural wavelength of the mode TM_{120} . The condition for resonance is: the total admittance at $r=r_2+0$ (looking into the iris) should be zero. And we have

$$y + jb_1 = 0, \quad (60)$$

where y is the relative input admittance at $r=r_2$ of a radial transmission line open-circuited at $r=0$, and y is given by⁸

$$y = -j[J_1'(kr)/J_1(kr)] \quad (61)$$

or, substituting in Eq. (60), we have

$$\frac{J_1[2\pi r/\lambda]}{J_1'[2\pi r/\lambda]} = +\frac{1}{b_1}.$$

To solve for r/λ we introduce a small dimensionless number ϵ . We put

$$r_2 = (7.02/2\pi)\lambda[1 + (\epsilon/7.02)], \quad (62)$$

and we have

$$J_1(7.02 + \epsilon)/J_1'(7.02 + \epsilon) = +1/b_1. \quad (63)$$

Taking the Taylor series expansion of the bessel functions of the first order, at the neighborhood of the second root 7.02, for small values of ϵ , we have

$$\epsilon = 1/(b_1 - 1/7.02). \quad (64)$$

Having corrected the radius r_2 for the TM_{120} mode, we have to adjust the length in order to make the modes TM_{111} and TE_{011} in tune with the former mode. To do this, we take, for the TM_{111} and the TE_{011} ,

$$\lambda = 2\pi[(3.832/a)^2 + (\pi^2/F)^2]^{-1/2}, \quad (65)$$

and to make $\Delta\lambda=0$, we must have

$$\Delta l = (3.832/\pi)^2(l/a)^2(\Delta a/a) \quad (66)$$

or

$$\Delta l/l = (3.832/\pi)^2(l/a)^2(\Delta a/a).$$

However, for each mode there is still the frequency change due to the perturbation screws and one or two perturbation holes. Thus, for the TM_{120} there are four screws and one hole. For both the TM_{111} and TE_{011} there are four screws and two holes. The fractional frequency changes of the three modes TM_{120} , TM_{111} , and TE_{011} are therefore, respectively, as follows:

$$(\delta\omega/\omega)_1 = 0.525k_{12} + 0.0965k_{23}, \\ (\delta\omega/\omega)_2 = 0.128k_{12} + 0.51k_{23} - (0.0326/|b|), \quad (67) \\ (\delta\omega/\omega)_3 = +0.24k_{23} + (0.0022/|b|).$$

When examined in this form, the fractional frequency changes, Eqs. (67), are seen to tend to be positive for the TM_{120} and the TE_{011} modes, but negative for the TM_{111} mode. By shortening the length of the cavity, the resonant frequencies of the TM_{111} and the TE_{011} modes can be raised toward that of the TM_{120} .

⁸ Montgomery, Dicke, and Purcell, *Principles of Microwave Circuits* (McGraw-Hill Book Company, Inc., New York, 1948), M. I. T. Radiation Laboratory Series, Vol. 8.

Thus, if we take

$$\Delta l/l = -(2l/\lambda)(\Delta\omega/\omega), \quad (68)$$

where $\Delta\omega/\omega$ is taken as

$$\Delta\omega/\omega = (\delta\omega/\omega)_1 - \frac{1}{2}[(\delta\omega/\omega)_2 + (\delta\omega/\omega)_3], \quad (69)$$

the three modes are brought closer together.

The final dimension of this 5-mode filter is given as follows:

$$D = (7.016/\pi)[\lambda + (\epsilon/7.02)], \\ l = 0.2673D[1 + 0.0606\epsilon - (2l/\lambda)^2(\Delta\omega/\omega)]. \quad (70)$$

The only problem which remains to be solved now is to find the value of b_1 from the lumped circuit equivalent prototype structure. Now looking into the cavity from the rectangular guide, the actual value of the open-circuited admittance is

$$B_{11} = Y_e(kr)[b_1 - [J_1'(kr)/J_1(kr)]], \quad k = 2\pi/\lambda. \quad (71)$$

The slope of B_{11} at its zero, after being simplified by putting in (61), is

$$dB_{11}/d\omega|_{\omega_0} = Y_e(ka)(7.02k^2/\omega_0). \quad (72)$$

If now we take the first equation of (33), and then substitute the value of X_1 given by (15), remembering the normalization condition (35), we have

$$b_1 = \{(\omega_0/\omega)(2C_1/7.016)\}^{1/2}\{Y_{10}TE/Y_e\}^{1/2}, \quad (73)$$

where ω_0/ω is ratio of the mid-frequency to the band width, C_1 is given in the prototype structure, and 7.02 is the second root of $J_1(x)$.

6. Experimental Models

Filter No. 1. A 2-mode filter, a single coupling screw, No. 4/40, $\omega_0/\omega = 400$, $\omega_0 = 9375$ mc, $\lambda = 3.20$ cm = 1.26 in., $D = \frac{1}{8}$ in., pass-band tolerance 3 db, $R = 0.172$, $C_1 = 3.140$ (Eq. (17)) $|b_1| = 14.95$ (Eq. (36)), d_1 (diameter of the input and output iris) = 0.319 in. (Eq.

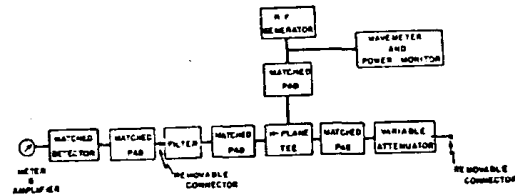


FIG. 12. Schematic experimental setup.

(42)), $l = 1.005$ in. (Eq. (52)), $k = 0.914 V_s/V$ (V_s , volume of the coupling screw, Eq. (10)), $k = 1.92 \times 10^{-3}$ (Eq. (38)).

Filter No. 2. A 3-mode filter, $\lambda = 3.20$ cm, $\omega_0/\omega = 400$, $\omega_0 = 9375$ mc, pass-band tolerance 1 db, $D = 0.965$ in. (point A, Fig. 1), $L_2 = 1$, $C_1 = 2$ (Eq. (19)), $k = 1.77 \times 10^{-3}$, $|b_1| = 13.3$, $d_1 = 0.327$ in., $l = 0.995$ in. (Eq. (59)).

Filter No. 3. A 5-mode filter, $\lambda = 3.20$ cm, $\omega_0/\omega = 454$, $w = 20.7$ mc, $D = 2.790$ in., $l = 0.755$ in. (Eq. (70)), $|b_1| = 16.56$ (Eq. (73)), $C_1 = C_3 = 2.1186$, $C_2 = 2.9698$, $L_2 = 1.0964$ (Fig. 9), $k_{12} = k_{43} = 1.445 \times 10^{-3}$, $k_{23} = k_{34} = 1.220 \times 10^{-3}$ (Eq. (38)), $k_{12} = 5.85 V_1/V$, $k_{23} = 1.132 V_2/V$ (Eqs. (11), (12)), $d = 0.382$ in. (Eq. (43)).

7. Measurements

In the experimental setup of Fig. 12, and H -plane